

IMECE2007-41344

THE EFFECTS OF TIBIOFEMORAL ANGLE AND BODY WEIGHT ON THE STRESS FIELD IN THE KNEE JOINT

Nicholas H. Yang
Northeastern University
Boston, MA 02115

H. Nayeb-Hashemi*
Northeastern University
Boston, MA 02115

Paul K. Canavan
Northeastern University
Boston, MA 02115

ABSTRACT

Osteoarthritis (OA) is a degenerative disease of articular cartilage that may lead to pain, limited mobility and joint deformation. It has been reported that abnormal stresses and irregular stress distribution may lead to the initiation and progression of OA. Body weight and the frontal plane tibiofemoral angle are two biomechanical factors which could lead to abnormal stresses and irregular stress distribution at the knee. The tibiofemoral angle is defined as the angle made by the intersection of the mechanical axis of the tibia with the mechanical axis of the femur in the frontal plane. In this study, reflective markers were placed on the subjects' lower extremity bony landmarks and tracked using motion analysis. Motion analysis data and force platform data were collected together during single-leg stance, double-leg stance and walking gait from three healthy subjects with no history of osteoarthritis (OA), one with normal tibiofemoral angle (7.67°), one with varus (bow-legged) angle (0.20°) and one with valgus (knocked-knee) angle (10.34°). The resultant moment and forces in the knee were derived from the data of the motion analysis and force platform experiments using inverse dynamics. The results showed that Subject 1 (0.20° valgus) had a varus moment of 0.38 N-m/kg, during single-leg stance, a varus moment of 0.036 N-m/kg during static double-leg stance and a maximum varus moment of 0.49 N-m/kg during the stance phase of the gait cycle. Subject 2 (7.67° valgus tibiofemoral angle) had a varus moment of 0.31 N-m/kg, during single-leg stance, a valgus moment of 0.046 N-m/kg during static double-leg stance and a maximum varus moment of 0.37 N-m/kg during the stance phase of the gait cycle. Subject 3 (10.34° valgus tibiofemoral angle) had a varus moment of 0.30 N-m/kg, during single-leg stance, a valgus moment of 0.040 N-m/kg during static double-leg stance and a maximum varus moment of 0.34 N-m/kg during the stance phase of the gait cycle. In general, the results show that the

varus moment at the knee joint increased with varus knee alignment in static single-leg stance and gait.

The results of the motion analysis were used to obtain the knee joint contact stress by finite element analysis (FEA). Three-dimensional (3-D) knee models were constructed with sagittal view MRI of the knee. The knee model included the bony geometry of the knee, the femoral and tibial articular cartilage, the lateral and medial menisci and the cruciate and the collateral ligaments. In initial FEA simulations, bones were modeled as rigid, articular cartilage was modeled as isotropic elastic, menisci were modeled as transversely isotropic elastic, and the ligaments were modeled as 1-D nonlinear springs. The material properties of the different knee components were taken from previously published literature of validated FEA models. The results showed that applying the axial load and varus moment determined from the motion analysis to the FEA model Subject 1 had a Von Mises stress of 1.71 MPa at the tibial cartilage while Subjects 2 and 3 both had Von Mises stresses of approximately 1.191 MPa. The results show that individuals with varus alignment at the knee will be exposed to greater stress at the medial compartment of the articular cartilage of the tibia due to the increased varus moment that occurs during single leg support.

INTRODUCTION

Osteoarthritis (OA) is a degenerative disease of articular cartilage that affects millions of people [1]. Its symptoms include limited mobility, pain and joint deformity [2]. It is common belief that both systemic and biomechanical factors contribute to OA development in a joint. The systemic factors, such as age, sex, racial characteristics and genetics, are considered as the foundation for cartilage properties [2-5]. However, the local biomechanical factors (joint loading, joint injury, weight bearing, joint deformity, meniscectomy, alignment, etc.) may severely affect initiation and progression

* Corresponding author; hamid@coe.neu.edu

of OA [2-14]. Body weight and frontal plane varus/valgus (tibiofemoral) knee alignment are two biomechanical factors that have been shown to affect the stress distribution at the knee joint (15-18). Increased body weight increases the mechanical loading at the knee joint. The clinical studies of individuals with prior knee OA symptoms have shown that body mass index (BMI) and tibiofemoral alignment increases the risk of knee OA progression (1, 7, 12, 13).

The knee joint alignment is measured by the angle formed by the intersection of the mechanical axes of the femur and the tibia, Fig. 1 [19]. Based on various methods used to measure tibiofemoral alignment, the angle for a normal person has been reported to be 5° to 7° valgus [19]. Deviation from these angles results in a knee joint with a valgus and varus condition. It has been shown that for a normally aligned knee, the medial compartment of the tibia is exposed to a higher stress than the lateral compartment of the tibia [15-18]. A varus knee will have a moment that increases the loading on the medial compartment of the knee and a valgus knee will have a moment that increases the loading on the lateral compartment of the knee. Therefore, understanding the stress and strain field in the cartilage is imperative in determining preventive measure to combat the negative effect of knee joint alignment on initiation and progression of damage to articular cartilage. FEA has been widely used to determine contact kinematics, stress distribution and loading in healthy and injured knees. The goal of this study is to utilize 3-D FEA knee models that can be used to determine the change in the stress and strain at the knee due to increased weight and tibiofemoral angle. Three subjects with different weight and tibiofemoral alignment performed static single-leg stance, static double-leg stance and walking gait. A motion analysis and force platform system recorded the kinematics of the leg and ground reactions in order to find the reactions at the knee joint using inverse dynamics. The reactions were used to define the loading conditions in the FEA simulations. The loading conditions include the loads and moments at the knee including the varus/valgus moment which is dependent on the frontal tibiofemoral angle.

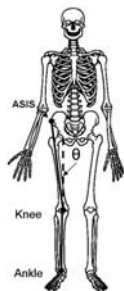


Figure 1 - The mechanical axis of the tibia is shown by a line from the ankle to the knee and the mechanical axis of the femur is show by a line from the knee to the anterior superior iliac spine (ASIS). A varus knee can be described as “bow-legged” ($\theta < 7^\circ$) and a valgus knee can be described as “knocked-kneed” ($\theta > 7^\circ$).

Finite Element Investigation

Existing 3-D FEA knee models have been either constructed from magnetic resonance images (MRI) or from computed tomography images (CT). The accuracy of these techniques in constructing a solid model of the knee joint has been investigated by Li et al [20]. They observed a variation of less than 8% in the cartilage thickness when constructing a solid model of the knee joint. Furthermore, Li et al [21, 22] investigated the change in contact stresses due to change in material properties of the cartilage and the ACL stiffness. Haut Donahue et al [23, 24] and Zielinska and Haut Donahue [25] created 3-D knee models to compare the contact stresses found from FEA simulations to those obtained experimentally using a cadaveric knee.

Since the stiffness of bone is much greater than that of the surrounding soft tissue within the knee, bones have been modeled as rigid components in FEA studies [20-25, 29, 30]. Haut Donahue et al verified that assuming bone as rigid material was not only valid but also reduced computational time [21].

Some FEA simulations have modeled the cartilage as linear elastic since for short loading durations the mechanical response of cartilage does not vary significantly with time [20-25]. However, since cartilage is a biphasic material consisting of a porous, permeable matrix with an interstitial fluid phase, various investigations have modeled cartilage as a poroelastic material. [26-30]. Yao et al [29] showed that modeling the cartilage as isotropic elastic, isotropic poroelastic, and transversely isotropic poroelastic produce different contact results.

In addition to the proposed material models for cartilage, various material models have been considered for meniscus and ligaments. Menisci have been modeled as nonlinear spring [20-22], as transversely isotropic elastic material [23-25], and as transversely isotropic poroelastic material [26-30]. The ligaments have been modeled as nonlinear spring elements within their representative bundles as well as solid elements [31].

The goal of this research is to develop a 3-D FEA knee model to observe the change in the stresses at the articular cartilage due to body weight and tibiofemoral angle. The material properties of the different components of the knee are adopted from previously validated FEA models.

METHODS

For this investigation, three healthy individuals with no history of knee OA or knee injury were used. The subjects consisted of one male and two females with the age range of 21-25 years old. Institutional Review Board approval was obtained prior to conducting the experiments.

Motion Analysis and Force Platform Experiments

Data was collected with a motion analysis system (Evert 5.0, Motion Analysis Corporation, Santa Rosa, CA) and two force platforms (Advanced Mechanical Technology, Inc. (AMTI), models OR6-6-2000, OR6-7-2000, Waltham, MA). The motion analysis consists of 6 cameras recordings at a frequency of 120 Hz. The motion analysis system records the kinematic data (position, velocity and acceleration) of reflective markers placed at bony landmarks on the body that define joint and center of mass (COM) locations. Reflective markers were placed on the (1) anterior superior iliac spine (ASIS), (2) the greater trochanter (3, 4) the lateral and medial femoral condyles, (5, 6) lateral and medial malleolus and (7) the head of the second metatarsal and (8) the S2, Fig. 2. The position of the knee and ankle joint were defined as the average position of the lateral and medial femoral condyles and malleoli, respectively, and defined with virtual markers in the motion analysis software. Virtual markers also define the position of the COM of the foot, leg and thigh section, Fig 2B. The locations of the COM of the different segments were defined as functions of the length of the different segment from statistical anthropometric data [32].

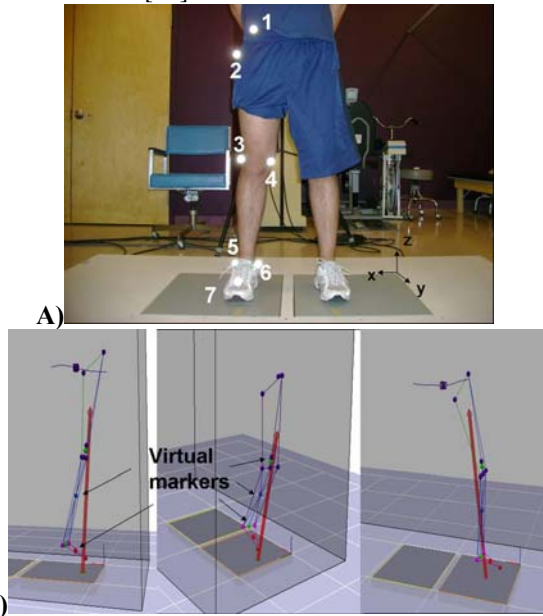


Figure 2 – A) Markers set used in motion analysis experiment with the marker #8 on the S2. B) Markers set including virtual markers representing the joint location and COM position.

The force platform configuration consisted of two platforms, 6.0 cm apart, one for each leg. The size of the force platforms are 51.0 x 48.0 cm, Fig. 2. The ground reactions and the location of where they act, center of pressure (COP), were found by the force platform. The subjects were asked to perform three trials of static double-leg stance for 10 seconds, static single-leg stance for 10 seconds and walking for 5 m.

With the ground reactions and kinematic data of the different joints and COM of the different segments, the reaction

force and moments on the knee joint were evaluated. Although many muscles acting at different locations contribute to the force and moments at each joint, the resultant forces and moments of the muscles are defined at the center of the knee joint.

Tibiofemoral Angle

The mechanical axis of the tibia in the frontal plane is defined as a line from the center of the ankle to the center of the knee and the mechanical axis of the femur is defined as a line from the center of the knee to the ASIS, Fig. 3. The tibiofemoral angle θ is the angle created from the intersection of these two mechanical axes. The angle was assessed while the subjects were in double leg stance with the second metatarsal 30 cm apart. The standard position was used to ensure the tibia was vertical and facing forward with minimal rotation [15].



Figure 3 – Tibiofemoral angle defined by the marker set.

Resultant Forces and Moments

The data from the motion analysis and the force platform trials was used to find the reaction forces and moments at the ankle joint, knee joint and at the distal end of the femur. The lengths of each segment of the leg were approximated using the marker set. The mass, center of mass (COM) and mass moment of inertia about the COM for each segment were found using statistical anthropometric data [32]. The mass for the foot, leg and thigh were found as a percentage of the total body mass M_b as $0.0145M_b$, $0.0465M_b$ and $0.100M_b$, respectively. The COM from the proximal end of each segment is [32]

$$\begin{aligned} COM_{foot} &= 0.50 * L_{foot} \\ COM_{leg} &= 0.433 * L_{leg} \\ COM_{thigh} &= 0.433 * L_{thigh} \end{aligned} \quad (1)$$

where L is the length of the respective segment.

The mass moment of inertia I_o about the center of mass for each segment about the x-axis is [32]

$$I_o = m\rho_o^2 \quad (2)$$

where m is the mass of the segment and ρ_o is the radius of gyration of the respective segment. The radius of gyration for the different segments is [32]

$$\begin{aligned} \rho_{o,foot} &= 0.475 * L_{foot} \\ \rho_{o,leg} &= 0.302 * L_{leg} \\ \rho_{o,thigh} &= 0.323 * L_{thigh} \end{aligned} \quad (3)$$

For an arbitrary segment, the equations used to find the forces and moments can be presented as [32]

$$\begin{aligned} \sum F_x &= ma_x \\ \sum F_y &= ma_y \\ \sum F_z &= ma_z \\ \sum M_x &= I_x \alpha_x + (I_z - I_y) \omega_y \omega_z \\ \sum M_y &= I_y \alpha_y + (I_x - I_z) \omega_x \omega_z \\ \sum M_z &= I_z \alpha_z + (I_x - I_y) \omega_x \omega_y \end{aligned} \quad (4)$$

where I_x , I_y , and I_z are the mass moments of inertia about the COM, a_x , a_y and a_z are the accelerations, α_x , α_y and α_z are the angular accelerations and ω_x , ω_y and ω_z are the angular velocities acting at the COM and determined from the motion analysis data. For static analysis all acceleration and velocities were zero. The coordinate system was defined as the z-axis normal to the force platform and the y-axis normal the frontal plane of the subjects. Considering this system, it can be assumed that there is no linear motion in the x-direction and no rotation about the y-axis and z-axis, $a_x = a_z = \alpha_x = \alpha_y = \alpha_z = \omega_x = \omega_y = \omega_z = 0$. Furthermore, with these assumptions, only the mass moment of inertia about the x-axis is needed to solve Eq. 4. Therefore, Eq. 4 reduces to

$$\begin{aligned} \sum F_x &= 0 \\ \sum F_y &= ma_y \\ \sum F_z &= ma_z \\ \sum M_x &= I_x \alpha_x \\ \sum M_y &= 0 \\ \sum M_z &= 0 \end{aligned} \quad (5)$$

Figure 4 shows the link segment models used to find the reactions at the different joints. Line $AC_F T$ represents the foot segment and (x_{ac}, y_{ac}, z_{ac}) are the distances from the COM of the foot to the center of the ankle joint and (x_{gc}, y_{gc}, z_{gc}) are

the distances from the ground reactions to the center of mass of the foot, Fig. 4A. The linear accelerations a_{yf} and a_{zf} , the angular velocity ω_{xf} and the angular acceleration α_{xf} act at the center of mass of the foot. The unknown reactions at the ankle [F_{ax} F_{ay} F_{az} M_{ax} M_{ay} M_{az}] are found for single-leg stance, double-leg stance and as a function of the gait cycle from heel-strike to toe-off.

The reactions at the knee are calculated considering the reactions at the ankle and the accelerations that act at the COM of the leg. The segment link model of the leg is shown in Fig 4B. The line $AC_L K$ represents the segment of the leg. The distances from the ankle to center of mass of the leg are (x_{ac}, y_{ac}, z_{ac}) and the distances from the center of mass of the leg to the knee are (x_{kc}, y_{kc}, z_{kc}) . The linear accelerations at the knee are a_{yl} and a_{zl} , and the angular velocity and acceleration are ω_{xl} and α_{xl} , respectively. The unknown reactions at the knee [F_{kx} F_{ky} F_{kz} M_{kx} M_{ky} M_{kz}] are found for single-leg stance, double-leg stance and as a function of the gait cycle from heel-strike to toe-off.

In the FEA model, the reactions are applied to the distal end of the femur while the tibia is fixed in place. The femur is cut approximately 60 mm above the knee in the FEA model. Assuming a constant mass distribution throughout the thigh, L_{thigh} is defined as the length of the femur section in the FEA model and is used to define the percentage of mass, COM and moment of inertia about the COM of the thigh section. The mass of the thigh section is

$$m_{thigh} = 0.100M_b * \left(\frac{L_{thigh}}{L_T} \right) \quad (6)$$

where L_T is the length of the thigh from the center of knee to the greater trochanter.

Figure 4C shows the link segment of the thigh section and the reactions at the knee. The angular acceleration α_{xt} of the thigh and the orientation of the thigh are used to find a_{yt} and a_{zt} acting at the COM of the thigh section. The distances from the COM of the thigh section and the top of the cut are (x_{ct}, y_{ct}, z_{ct}) and the distances from the knee to the COM of the thigh section are (x_{kc}, y_{kc}, z_{kc}) . The reactions at the distal end of the thigh [F_{tx} F_{ty} F_{tz} M_{tx} M_{ty} M_{tz}] are calculated and applied to the FEA model to simulate stance and the gait cycle.

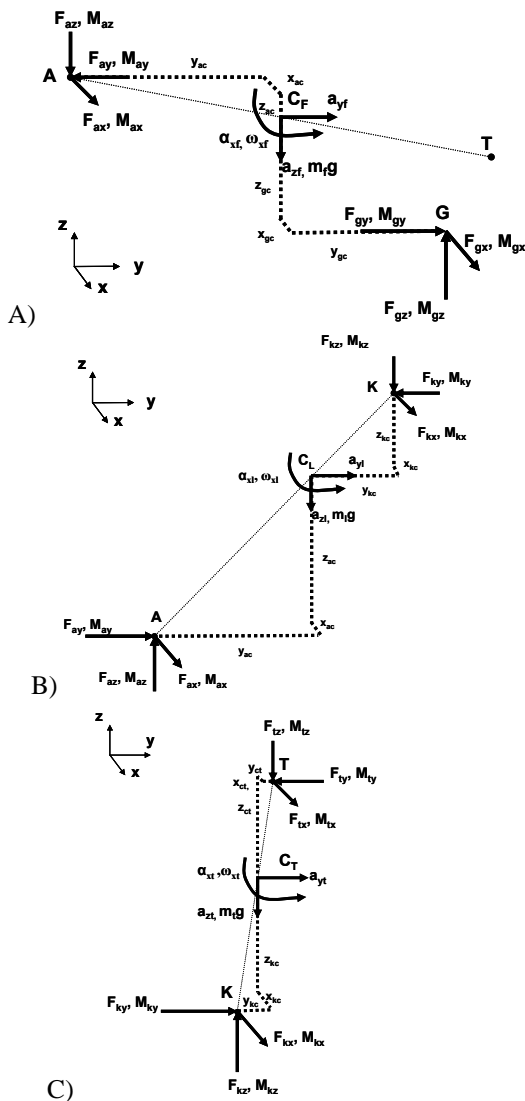


Figure 4 - Link segment model representing the A) foot, B) leg and C) thigh section.

Three-Dimensional FEA Model

3-D FEA models were created from the sagittal view magnetic resonance images (MRI) of the knee. The MRI were obtained at the Weymouth MRI center located in Weymouth, MA. The MRI were obtained in the early morning and the subjects did not participate in any strenuous activity prior to the scans. The MRI were taken of the subject in the supine, non-load bearing position. Subjects were rested with no load bearing for twenty minutes before the MRI were taken. For these initial FEA simulations, the axial loads and varus moments were applied to a 3-D model created from MRI of an unknown subject. In future investigations, the subject specific geometry will be incorporated to the model.

The 2-D images were loaded into the solid modeling program Rhinoceros (Rhinoceros 3.0, Seattle, Washington). The boundaries of the bones, cartilage and menisci were

digitized and 3-D point cloud models were constructed by aligning each 2-D segment in its respective position. The 3-D point cloud defines the 3-D surface geometry of the individual knee components used in the FEA simulations, Fig. 5. The ligaments were modeled as non-linear springs. The insertion sites to the bone are obtained from the MRI and incorporated into the 3-D geometry when applying the ligaments to the FEA model, Fig. 6.

This initial FEA investigation was to determine the effect of combination of the axial load and varus moment, derived from kinematics analysis, on the stress field on the tibial plateau. The axial load from the different subjects will be applied to the model to determine the change in the maximum Von Mises stress at the tibial plateau due to the increase weight of the subjects. The varus moment will then be applied along with the axial load to determine the change in the stress field at the articular cartilage.

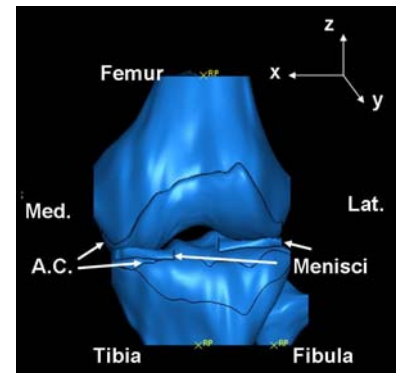


Figure 5 – Anterior view of the three dimensional FEA model of the left knee created from MRI. Included in the model are the femur, tibia, fibula, articular cartilage (A.C.) and lateral and medial menisci.

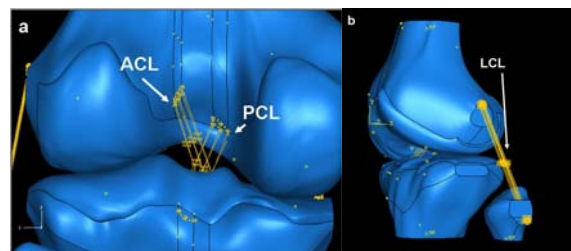


Figure 6 – (a) Posterior view of the left knee and the non-linear spring element representation of the ACL and the PCL in the FEA model and (b) representation of the LCL in the FEA model.

FINITE ELEMENT ANALYSIS

The 3-D knee model was exported into the finite element software package, ABAQUS (ABAQUS/CAE 6.5, ABAQUS, Inc., Pawtucket, RI). The material properties are assigned to the different components of the knee based on previously published data. The loading conditions are defined based on the results of the motion analysis and force platform data.

Bones and Cartilage

For this initial investigation the articular cartilage is modeled as one layer elastic isotropic, which is rigidly attached to the bone surface. However, in our future investigations, the cartilage will be modeled as an isotropic poroelastic material and a transversely isotropic poroelastic material and the material properties that define this behavior will be taken from Wilson et al [26] and are listed in Table 1.

Cartilage : Isotropic elastic	$E = .69 \text{ MPa}, \nu = 0.018$
Cartilage: Isotropic poroelastic	$E = 0.69 \text{ MPa}, G = 0.34 \text{ MPa}, \nu = 0.018,$ $k = 3*10^{-15} \text{ m}^4/\text{Ns}, \Phi_m = 0.25$
Cartilage: Transversely Isotropic poroelastic	$E_x = E_y = 0.46 \text{ MPa}, E_z = 5.8 \text{ MPa}, \nu_{xy} = 0.0002, \nu_{yz} = 0$ $G_{xz} = 0.37 \text{ MPa}, k = 5.1*10^{-15} \text{ m}^4/\text{Ns}, \Phi_m = 0.25$

Table 1 – The properties used for modeling the articular cartilage in the FEA model.

Menisci

The menisci are modeled as transversely isotropic elastic. Similar to the cartilage, poroelastic properties will be considered in future investigations. The material properties of the menisci used in this investigation, and to be used in future investigation, are reported from Wilson et al [26], Table 2. The menisci are attached to the tibial plateau at the meniscal horns using a set of linear spring elements similar to the methods used by Donahue et al [23]. At each horn attachment, ten linear springs with a stiffness of 200 N/mm attach the horn to the tibial plateau. The total stiffness for each horn attachment is 2000 N/mm [23]. A transverse ligament, which attaches the anterior horns of the lateral and medial menisci, is modeled as a linear spring with a stiffness of 900 N/mm [23-25].

Meniscus: Transversely Isotropic elastic	$E_{\theta} = 100 \text{ MPa}, E_r = E_a = .075 \text{ MPa},$ $\nu_{rz} = 0.5, \nu_{r\theta} = \nu_{z\theta} = 0.0015$ $G_{r\theta} = G_{z\theta} = 2.0 \text{ MPa}, G_{rz} = 0.025 \text{ MPa}$
Meniscus: Transversely Isotropic poroelastic	$E_{\theta} = 100 \text{ MPa}, E_r = E_z = .075 \text{ MPa},$ $\nu_{rz} = 0.5, \nu_{r\theta} = \nu_{z\theta} = 0.0015$ $G_{r\theta} = G_{z\theta} = 2.0 \text{ MPa}, G_{rz} = 0.025 \text{ MPa}$ $k = 1.26*10^{-15} \text{ m}^4/\text{Ns}, \Phi_m = 0.75$

Table 2 - The properties used for modeling the menisci in the FEA model.

Ligaments

Ligaments are the connective tissue normally found within the body that attaches bones to other bones, providing stability and strength to the joint. Four major ligaments connect the femur and tibia: medial collateral ligament (MCL), lateral collateral ligament (LCL), anterior cruciate ligament (ACL) and the posterior cruciate ligament (PCL).

The force-displacement relationship used to model the ligaments as non-linear springs can be defined using the piecewise function [31]

$$f = \begin{cases} \frac{1}{4}k\varepsilon^2 / \varepsilon_l, & 0 \leq \varepsilon \leq 2\varepsilon_l \\ k(\varepsilon - \varepsilon_l), & \varepsilon > 2\varepsilon_l \\ 0, & \varepsilon < 0 \end{cases} \quad (7)$$

where f is the tensile force, k is a stiffness parameter, ε_l is the non-linear strain parameter obtained from previously published literature and ε is the strain in the ligaments. In this study, the ACL and PCL were modeled with an anterior bundle and a posterior bundle. The LCL and MCL were modeled with three bundles. The mechanical behavior of the springs representing the different bundles is shown in Table 3.

Ligament	Bundle	Stiffness parameter, k [N]	ε_r
Anterior Cruciate	anterior	5000	0.06
	posterior	5000	0.1
Posterior Cruciate	anterior	9000	-0.24
	posterior	9000	-0.03
Lateral Collateral	anterior	2000	-0.25
	superior	2000	-0.05
	posterior	2000	0.08
Medial Collateral	anterior	2750	0.04
	inferior	2750	0.04
	posterior	2750	0.03

Table 3 – Material properties of the ligaments used in the FEA model.

RESULTS AND DISCUSSION

Table 4 shows the weight and tibiofemoral angle in the frontal plane for three subjects. All the angles are valgus (measured medial to the knee) and Subject 1 is relatively varus (bow-legged), Subject 2 has relatively normal alignment and Subject 3 is relative valgus alignment (knock-kneed).

Subject	1 (Varus)	2 (Normal)	3 (Valgus)
Tibiofemoral angle (Valgus)	0.20°	7.67°	10.34°
Weight (N)	640	725	714

Table 4 – The tibiofemoral angle and the weight of different subjects. Subject 1 is relative varus knee alignment, Subject 2 is relative normal knee alignment and subject 3 is relative valgus knee alignment.

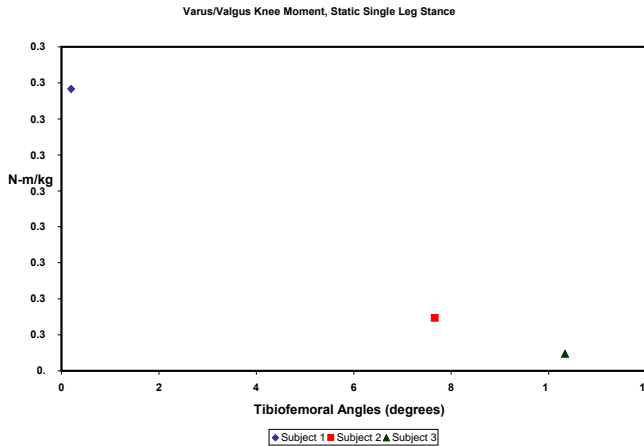


Figure 7 – Varus/valgus moment at the knee during static single-leg stance. A positive moment is varus and a negative moment is valgus.

Figure 7 shows the varus moment at the knee during static single-leg stance. The moment is normalized by the mass of the subjects. The magnitude of the varus moment is a function of the lateral position of the knee relative to the ankle. Figure 7 indicates that a larger tibiofemoral angle corresponds with a greater lateral distance from the ankle to the knee joint, which increases the varus moment at the knee. For all subjects, the knee was lateral to the ankle joint, creating a varus moment.

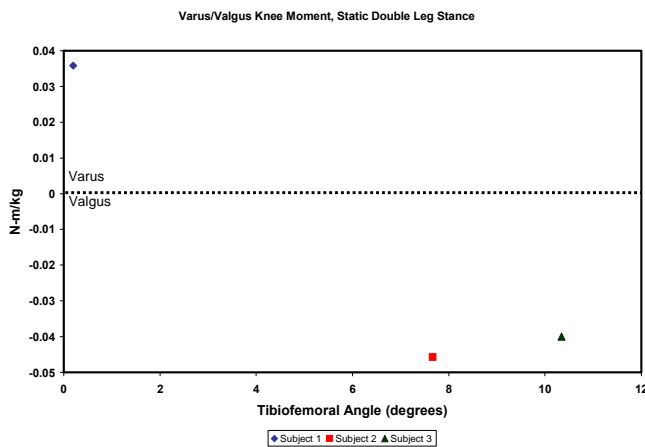


Figure 8 – Varus/valgus moment at the knee during static double-leg stance. A positive moment is varus and a negative moment is valgus.

Figure 8 shows the varus/valgus moments during double-leg stance. During double-leg stance, the knee moves medial to the ankle joint for Subject 2 and 3, creating a valgus moment at the knee. The knee position remains lateral to the

ankle joint for Subject 1, creating a varus moment during static double-leg stance.

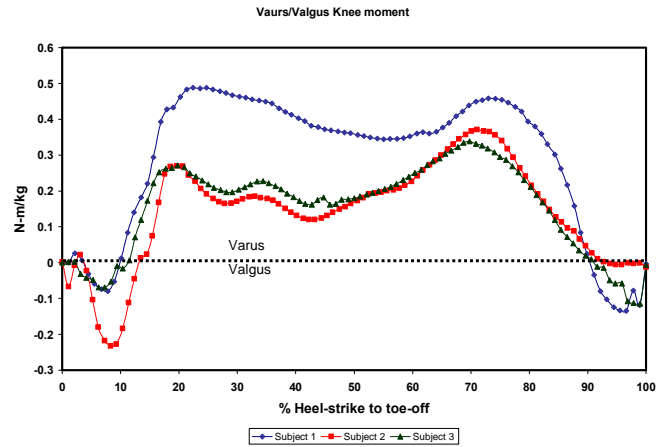


Figure 9 – Varus/valgus moment at the knee during the stance phase (heel-strike to toe-off) of the gait cycle. A positive moment is varus and a negative moment is valgus.

Figure 9 shows the varus/valgus moment of the three subjects during the stance phase of the gait cycle from heel-strike to toe-off. The varus (bow-legged) subject has the greatest varus knee moment during gait. Subject 2 and Subject 3 have comparable varus moment values but the initial valgus moments may be due to individual walking characteristics.

The results show that an individual with a varus tibiofemoral angle (bow-legged) will have a large varus moment during gait that will increase the loading on the medial compartment of the knee. The reactions at the knee could be applied to the FEA model to determine the stress distribution at the articular cartilage. Understanding the stress and strain at the joint is important because abnormal joint loading increases the risk of OA [14]. Furthermore, these results could be used by an expert to determine preventive measures such as strength training or the use of orthotics to minimize the varus moment to reduce the load on the medial compartment of the knee.

Initial FEA simulations were performed with isotropic elastic cartilage, transversely isotropic elastic menisci, rigid bones and 1-D non-linear springs for the ligaments. Two types of conditions were simulated: (1) axially loaded knee and (2) an axial load and a varus moment. The first case was to observe the effect of body weight on the maximum stress on the articular cartilage at the knee. The second case was to observe the effect of the varus moment on the maximum stress and stress distribution at the knee. The tibia and fibula were fixed in place and the femur was fixed at 0° flexion with all other degrees of freedom unconstrained while the loads were applied to the top of the femur section. The axial loads at the knee joint for the Subjects 1, 2 and 3 from the motion analysis and force platform data for single-leg static stance were 601 N, 681 N and 671 N. Applying these loads to the FEA models, the maximum Von Mises stress occurred on the medial tibial plateau was 0.514 MPa, 0.658 MPa and 0.639 MPa for Subject

1, Subject 2 and Subject 3, respectively. The results show with an axial load the stress at the tibial cartilage increases with increase in weight. Figure 9 shows that during the single-leg support of the stance phase (approximately 30%-60%) the average varus moment for Subject 1, Subject 2 and Subject 3 is approximately 15 N-m, 8.8 N-m, and 9 N-m, respectively. Applying the respective varus moment and the axial load for the different subjects to the FEA model shows the Von Mises stress on the medial compartment of the tibia increases to 1.710 MPa, 1.191 MPa and 1.192 MPa, respectively, while decreasing the stress distribution on the lateral compartment of the tibia, Fig. 10. The results show that individuals with varus alignment at the knee will be exposed to greater stress at the medial compartment of the articular cartilage of the tibia due to the increased varus moment that occurs during single leg support. This information could be used to determine preventive measures, such as the use of foot orthotics, proper footwear or strength training, to decrease the varus moment at the knee and thus the loading on the medial compartment of the knee in order to prevent the initiation or slow the progression of OA.

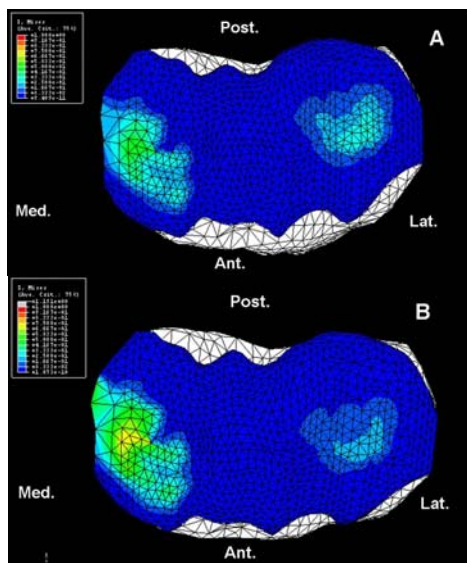


Figure 10 – The top view of the tibia and the cartilage showing the Von Mises stress distribution for A) axially loaded knee and B) axially loaded knee with a varus moment.

CONCLUSION

The purpose of this research is to develop 3-D FEA models of the knee in order to apply reactions found from motion analysis and force platform experiments to find the stress and strain distribution at the articular cartilage of the knee. The influence of the tibiofemoral angle and body weight on the stress in the knee is also investigated. The results showed that a relative varus tibiofemoral alignment (bow-legged) increased the varus moment at the knee during static single-leg stance and gait, which would lead to increased loading on the medial compartment of the knee. The FEA results showed that the stress in the articular cartilage of the

tibia increased on the medial compartment with increased varus moment. Future considerations of this work include poroelastic material properties, subject specific 3-D models to include the difference in knee geometry, and possibly parametric studies. The stress distribution at the knee from the FEA simulations could be used by experts to determine preventive measures such as strength training or the use of orthotics to prevent abnormal loading conditions and delay the initiation or slow the progression of OA.

REFERENCES

- [1] Sharma, L., Song, J., Felson, D.T., Cahue, S., Shamiyeh, E. and Dunlop, D.D., "The Role of Knee Alignment in Disease Progression and Functional Decline in Knee Osteoarthritis," *JAMA*, 2, **286**, 2001, pp. 188-195.
- [2] Arokoski, J.P.A., Jurvelin, J.S., Vaatainen, U. and Helminen, H.J., 2000, "Normal and Pathological Adaptations of Articular Cartilage to Joint Loading," *Scandinavian Journal of Medicine and Science in Sports*, **10**, pp. 186-198.
- [3] Sowers, M., 2001, "Epidemiology of Risk Factors for Osteoarthritis: Systemic Factors," *Current Opinion in Rheumatology*, **13**, pp. 447-451.
- [4] Felson, D.T. and Zhang, Y., 1998, "An Update on the Epidemiology of Knee and Hip Osteoarthritis with a View to Prevention," *Arthritis and Rheumatism*, **41**, no. 8, pp. 1343-1355.
- [5] Felson, D.T., Conference Chair, "Osteoarthritis: New Insights. Part 1: The Disease and its Risk Factors," *Ann Intern Med.*, pp. 635-646.
- [6] Sharma, L., 2001, "Local Factors in Osteoarthritis," *Current Opinion in Rheumatology*, **13**, pp. 441-446.
- [7] Sharma, L., Lou, C., Cahue, S. and Dunlop, D.D., 2000, "The Mechanism of the Effect of Obesity in Knee Osteoarthritis," *Arthritis and Rheumatism*, **43** No. 3, pp. 568-575.
- [8] Roos, E.M., 2005, "Joint Injury Causes Knee Osteoarthritis in Young Adults," *Current Opinion in Rheumatology*, **17**, pp. 195-200.
- [9] Cooper, C., Snow, S., McAlindon, T.E., Kellingray, S., Stuart, B., Coggon, D. and Dieppe, P.A., 2000, "Risk Factors of the Incidence and Progression of Radiographic Knee Osteoarthritis," *Arthritis and Rheumatism*, **43**, No. 5, pp. 995-1000.
- [10] Powell, A., Teichtahl, A.J., Wluka, A.E. and Cicuttini, F.M., 2005, "Obesity: A Preventable Risk Factor for Large Joint Osteoarthritis which may act through Biomechanical Factors," *British Journal of Sports Medicine*, **54**, pp. 4-5.
- [11] Englund M. and Lohmander, L.S., 2004, "Risk Factors for Symptomatic Knee Osteoarthritis Fifteen to Twenty-Two Years after Meniscectomy," *Arthritis and Rheumatism*, **50**, No. 9, pp. 2811-2819.
- [12] Cerejo, R., Dunlop, D.D., Cahue, S., Channin, D., Song, J. and Sharma, L., 2002, "The Influence of Alignment on Risk of Knee Osteoarthritis Progression According to Baseline Stage of Disease," *Arthritis and Rheumatism*, **46**, No. 10, pp. 2632-2636.

- [13] Felson, D.T., Goggins, J., Niu, J., Zhang, Y. and Hunter, D.J., 2004, "The effect of Body Weight on Progression of Knee Osteoarthritis is Dependent on Alignment," *Arthritis and Rheumatism*, **50**, No. 12, pp. 3904-3909.
- [14] Griffin, T.M. and Guilak, F., 2005, "The Role of Mechanical Loading in the Onset and Progression of Osteoarthritis," *Exercise and Sports Science Reviews*, **33**, no. 4, pp. 195-200.
- [15] Hsu, R.W.W., Himeno, S., Coventry, M.B. and Chao, E.Y.S., 1990, "Normal Axial Alignment of the Lower Extremity and Load-Bearing Distribution at the Knee," *Clinical Orthopedics and Related Research*, **255**, pp. 215-227.
- [16] Chao, E.Y.S., Neluheni, E.V.D., Hsu, R.W.W. and Paley, D., 1994, "Biomechanics of Malalignment," *Orthopedic Clinics of North America*, **25**, no. 4, pp. 379-386.
- [17] Johnson, F., Leitt, S. and Waugh, W., 1980, "The Distribution of Load across the Knee," *Journal of Bone and Joint Surgery - British Volume*, **62-B**, no. 3, pp. 346-349.
- [18] Bruns, J., Volkmer, M. and Luessenhop, S., 1993, "Pressure Distribution at the Knee Joint: Influence of Varus and Valgus Deviation without and with Ligament Dissection," *Arch Orthop Trauma Surg*, **133**, no. 1, pp. 12-19.
- [19] Karachalios, T., Sarangi, P.P. and Newman, J.H., 1994, "Severe Varus and Valgus Deformities Treated by Total Knee Arthroplasty," *The Journal of Bone and Joint Surgery*, **76**, pp. 938-942.
- [20] Li, G., Lopez, O. and Rubash, H., "Variability of a Three-Dimensional Finite Element Model Constructed Using Magnetic Resonance Images of a Knee for Joint Contact Stress Analysis," (2001), *Journal of Biomedical Engineering*, **123**, pp. 341-346.
- [21] Li, G., Gil, J., Kanamori, A. and Woo, S.L-Y., 1999, "A Validated Three-Dimensional Model of a Human Knee Joint," *Journal of Biomechanical Engineering*, **121**, pp. 657-662.
- [22] Li, G., Suggs, J. and Gill, T., 2002, "The Effect of Anterior Cruciate Ligament Injury on Knee Joint Function under a Simulated Muscle Load: A three-Dimensional Computational Simulation," *Annals of Biomedical Engineering*, **30**, pp. 713-720.
- [23] Haut Donahue, T.L., Hull, M.L., Rashid, M.M. and Jacobs, C.R., 2002, "A Finite Element Model of the Human Knee Joint for the Study of Tibio-Femoral Contact," *Journal of Biomechanical Engineering*, **124**, pp. 273-280.
- [24] Haut Donahue, T.L., Hull, M.L., Rashid, M.M. and Jacobs, C.R., 2002, "how the Stiffness of meniscal Attachments and meniscal material Properties affect Tibio-Femoral Contact Pressure Computed using a Validated Finite Element Model of the Human Knee Joint," *Journal of Biomechanical Engineering*, **36**, pp. 19-34.
- [25] Zielinska, B. and Hart Donahue, T.L., 2006, "3D Finite Element Model of Meniscectomy: Changes in Joint Contact Behavior," *Journal of Biomechanical Engineering*, **128**, pp. 115-123.
- [26] Wilson, W., van Rietbergen, B., van Donkelaar, C.C. and Huiskes, R., (2003) "Pathways of Load-Induced Cartilage Damage Causing Cartilage Degeneration in the Knee after Meniscectomy," *Journal of Biomechanics*, **36**, pp. 845-851.
- [27] Wilson, W., van Donkelaar, C.C., van Rietbergen, B., Ito, K. and Huiskes, R., 2003, "Stresses in the Local Collagen Network of Articular Cartilage: A Poroviscoelastic Fibril-Reinforced Finite Element Study," *Journal of Biomechanics*, **37**, pp. 357-366.
- [28] Wilson, W., van Donkelaar, C.C., van Rietbergen, B. and Huiskes, R., 2005, "The Role of Computational Models in the Search for the Mechanical Behavior and Damage Mechanisms of Articular Cartilage," *Medical Engineering & Physics*, **27**, pp. 810-826.
- [29] Yao, J., Salo, A.D., Barbu-McInnis, M., and Lerner, A.L., "Finite element modeling of knee joint contact pressures and comparison to magnetic resonance imaging of the loaded knee", *Proceedings of IMECE'03 2003 ASME International Mechanical Engineering Congress*, Washington, D.C., Nov. 15-21, 2003, pp. 247-248.
- [30] Zhang, H., Totterman, S., Perucchio, R., and Lerner, A. L., 1999, "Magnetic Resonance Image Based Three-Dimensional Poroviscoelastic Finite Element Model of Tibio-Menisco-Femoral Contact," *Proc. Annual Meeting of American Society of Biomechanics*, Vol. 23, Pittsburgh, PA.
- [31] Blankevoort, L., Kuiper, J.H., Huikes, R. and Grootenboer, H.J., 1991, "Articular Contact in a Three-Dimensional Model of the Knee," *Journal of Biomechanics*, **24** no. 11, pp. 1019-1031.
- [32] Winter, D.A., "Biomechanics and Motor control of Human Movement, 3rd Ed.," *John Wiley and Sons, Inc.*, 2005.